

PAPER • OPEN ACCESS

## The Effect of Seawater on The Strength, Microstructure and Elemental Distribution of Fly Ash/ Kaolin Based Underwater Geopolymer

To cite this article: Fakhryna Hannanee Ahmad Zaidi *et al* 2020 *IOP Conf. Ser.: Mater. Sci. Eng.* **864** 012014

View the [article online](#) for updates and enhancements.

You may also like

- [Fabrication, sinterability and characterization of non-colored and colored geopolymers with improved properties](#)  
S E Abo Sawan, M F Zawrah, R M Khattab *et al.*
- [Study on the effect of emulsifiers on the pore structures of geopolymer prepared by emulsion templating](#)  
Zhuangzhuang Wang and Duyou Lu
- [The effect of alkali activation solutions with different water glass/NaOH solution ratios on geopolymer composite materials](#)  
N Doan-Salamtimur, H Öznur Öz, A Bilgil *et al.*



**UNITED THROUGH SCIENCE & TECHNOLOGY**

 **The Electrochemical Society**  
Advancing solid state & electrochemical science & technology

**248th  
ECS Meeting**  
Chicago, IL  
October 12-16, 2025  
*Hilton Chicago*

**Science +  
Technology +  
YOU!**

**Register by  
September 22  
to save \$\$**

**REGISTER NOW**

# The Effect of Seawater on The Strength, Microstructure and Elemental Distribution of Fly Ash/ Kaolin Based Underwater Geopolymer

Fakhryna Hannanee Ahmad Zaidi<sup>1</sup>, Romisuhani Ahmad<sup>1</sup>, Mohd Mustafa Al Bakri Abdullah<sup>2</sup>, Wan Mastura<sup>1</sup> and Ahmad Syauqi<sup>1</sup>

<sup>1</sup>Center of Excellence Geopolymer & Green Technology (CEGeoGTech), Universiti Malaysia Perlis, Perlis, Malaysia.

<sup>2</sup>School of Material Engineering, Universiti Malaysia Perlis, Taman Muhibbah, 02600 Jejawi, Arau, Perlis, Malaysia.

E-mail: fakhryna0508@gmail.com

**Abstract.** Concrete in seawater is subjected to various aggressive constituents in seawater commonly sulphate, chloride and carbonate. This paper investigates the potential effects towards mechanical and physical properties of geopolymer when used as underwater concreting material. Besides identifying the microstructure using Scanning Electron Microscopy (SEM), the sample is also characterized using Synchrotron based micro X-Ray Fluorescence ( $\mu$ -XRF) to identify the elemental distribution that had occurred in the underwater geopolymer. Other essential properties for concrete such as compressive strength, water absorption and density were also determined. The compressive strength result indicates a slightly lower strength for underwater geopolymer (31.40 MPa) compared to normal geopolymer (35.91 MPa). Relevant to the strength, the water absorption and density also shows a slight difference between the geopolymer samples. The  $\mu$ -XRF analysis shows the presence of chlorine (Cl) element only for underwater geopolymer which indicates that there are chloride penetrations for underwater geopolymer. Additionally, other element distribution such as Silica (Si), Aluminum (Al) and Calcium (Ca) shows a different value when comparing normal geopolymer and underwater geopolymer. Despite the difference in elemental distribution between samples, geopolymer is proven to have the potential to be used as underwater material since it is able to retain at least 70% strength of the control sample.

## 1. Introduction

Concrete as a building material has been used for underwater works for many centuries. Placing concrete underwater is one of the most critical and complex operations that often determine the success or failure in the underwater structure [1]. Generally, one of the methods of placing underwater concrete is by Tremie method. A Tremie is simply a pipe long enough to reach the location of concrete deposition from above water [2]. Contrasting from typical concrete, concrete placed underwater is vulnerable to cement washout, laitance, segregation, cold joints, and water entrapment [3]. As a building structure, underwater concrete also requires high strength and durability to withstand the environment condition [4].

Nowadays, geopolymer materials are known as a new building material alternative to Portland cement due to its high strength and resistance to chemical attack [5-9]. Typically, Geopolymer is synthesized



by mixing aluminosilicate-reactive material with strong alkali solution such as sodium hydroxide (NaOH) and sodium silicate [10-12]. Due to the high content of silica and aluminium, fly ash is nowadays utilized to produce geopolymer material [13-16]. There are 2 types of fly ash, class C and class F classified by the total element of Si, Fe and Al [17-19]. Typically, low calcium system geopolymer such as class F fly ash which consist mainly of Si and Al provides aluminosilicate hydrate (N-A-S-H) as the main reaction products while high calcium system geopolymer such as class C fly ash provides calcium silicate hydrate (C-S-H), calcium aluminosilicate hydrate (C-A-S-H) and sodium aluminosilicate hydrate (N-A-S-H) as the main reaction products [20, 21]. The class c fly ash, also known as high calcium fly ash display different properties compared to class F fly ash where higher calcium content provides higher strength and shorter setting time. Due to the time taken for mixing and curing, there is a need to retard the setting time for more efficient mixing, pouring and geopolymerization. Thus, kaolin is added to help prolonged the setting time and gives extra Si and Al content for geopolymerization [22, 23].

While there is a few research related to geopolymer for underwater concreting, this research intends to identify the properties of geopolymer used for underwater concreting in seawater. The difference of mechanical properties and physical properties such as morphology and elemental distribution is identified in this paper.

## 2. Experimental Method

### 2.1. Raw Material

The fly ash used is attained from Manjung Power Plant, Lumut, Perak that is of low calcium, Class C is used as the base material of geopolymer and is equivalent to ASTM C618. While kaolin used in this study is supplied by Associated Kaolin Industries Malaysia as Si-Al sources materials. The chemical composition of fly ash and kaolin obtained from the analysis as tabulated in Table 1. The sodium hydroxide (NaOH) powder was of caustic soda micropearls and 99% purity with the brand name of Formosoda-P. The sodium silicate ( $\text{Na}_2\text{SiO}_3$ ) solution with a chemical composition of 30.1%  $\text{SiO}_2$ , 9.4%  $\text{Na}_2\text{O}$  and 60.5%  $\text{H}_2\text{O}$  was supplied by South Pacific Chemicals Industries Sdn. Bhd., Malaysia.

**Table 1.** XRF analysis of Fly ash class C and Kaolin powder

Element	$\text{SiO}_2$	$\text{Al}_2\text{O}_3$	CaO	$\text{Fe}_2\text{O}_3$	$\text{TiO}_2$	$\text{K}_2\text{O}$	SrO
<b>Kaolin</b>	54.0	31.7	-	4.89	1.41	6.05	-
<b>Fly Ash</b>	31.4	13.2	23.3	25.44	1.00	1.59	0.177

### 2.2. Sample Preparation

All geopolymer paste are made using raw fly ash and kaolin with the same design using 12M of sodium hydroxide, 2.5 ratio of alkaline activator and 2.0 ratio of solid to liquid. The method used for underwater geopolymer is by Tremie method. Each of sample is further tested for its mechanical and physical properties.

### 2.3. Testing

#### 2.3.1 In-Situ Epoxidation Micro X-Ray Fluorescence ( $\mu$ -XRF)

The micro beam energy dispersive X-ray fluorescence spectroscopy ( $\mu$ -XRF) based Synchrotron radiation source located at the Beamline 6 of Synchrotron Light Research Institute (SLRI), Bangkok, Thailand was applied for identifying the elemental distribution. The range of beam size used in the facilities was 2keV~20keV. The result of  $\mu$ -XRF was illustrated using PyMca software. The setting for both sample is tabulated according to table 2. X-ray fluorescence spectroscopy ( $\mu$ -XRF) based Synchrotron radiation source located at the Beamline 6 of Synchrotron Light Research Institute (SLRI), Bangkok, Thailand was applied for identifying the elemental distribution. The range of beam size used

in the facilities was 2keV~20keV. The result of  $\mu$ -XRF was illustrated using PyMca software. The setting for both sample is tabulated according to Table 2.

**Table 2.** Summary of  $\mu$ -XRF parameters.

Parameter	Value
Total scan point	1225
Dead time	25 %
Exposure time	3 s
Atmosphere	Helium

### 2.3.2 Compressive Strength

The cubic moulds of size 50mm samples were used for compressive strength testing according to ASTM C109/C109M – 16a by using Instron machine series 5569 Mechanical Tester after 28 days of exposure. The specimens were coated using Auto Fine Coater model JEOL JFC 1600 prior to examination.

### 2.3.3 Density

The density of these resulted geopolymer was conducted as according to BS EN12390-7 thus calculated according to the equation (1) below.

$$\text{Density, } \rho = \frac{\text{Mass, } M}{\text{Volume, } V} \quad (1)$$

### 2.3.4 Water Absorption

The water absorption test has been conducted according to the ASTM C140-12 standard. The formula to identify the water intake is according to the equation (2).

$$\text{Water absorption} = \frac{W_s - W_d}{W_d} \times 100 \quad (2)$$

Where:

Ws = saturated weight of samples (g)

Wd = oven-dry weight of samples (g)

### 2.3.5 Scanning Electron Microscopy (SEM)

JSM-6460LA model Scanning electron microscope (JEOL) was performed to reveal the microstructure of fly ash based geopolymers for each different pouring method.

### 2.3.6 Fourier Transform Infrared Spectroscopy (FTIR)

Perkin Elmer FTIR Spectrum RX1 Spectrometer was used to evaluate the functional group of the sample. The geopolymer samples were crushed small enough to fit the mould for scanning.

## 3. Results and Discussions

### 3.1. Compressive Strength, Water absorption and Density

Table 3 shows the result of compressive strength, water absorption and density of both underwater geopolymer and controlled geopolymer. Given that the underwater geopolymer are poured directly under water and let to cure, the sample is observed to gives a slightly lower (46.71MPa) compressive strength compared to control geopolymer (50.76MPa). Hence the underwater geopolymer are able to retain about 92.02% of the control geopolymer thus proves the ability of geopolymer for underwater concreting in terms of strength.

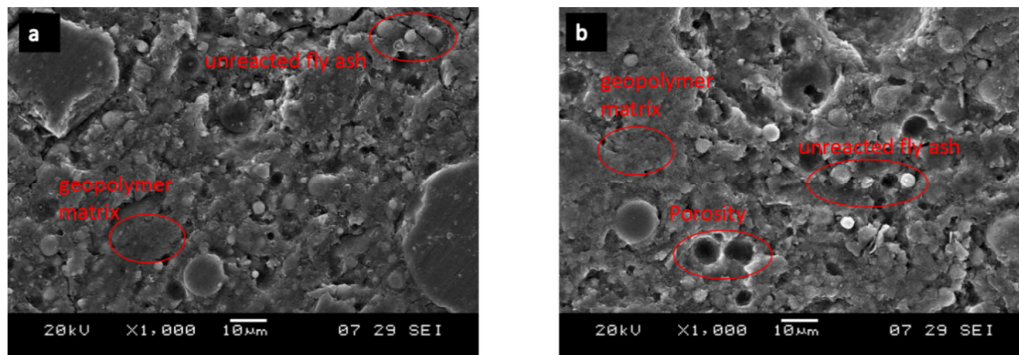
**Table 3.** Compressive strength, water absorption and density of samples.

	Underwater Geopolymer	Control Geopolymer
Compressive Strength (MPa)	46.71	50.76
Water Absorption (%)	0.17	0.1
Density (kg/m <sup>3</sup> )	2082.92	2168.08

The ingress of water can deteriorates the durability of concrete and mortar [24] thus water absorption testing is used to estimate the maximum amount of water that can be absorbed by dry specimen. Relevant to the compressive strength, the water absorption for underwater geopolymer (0.17%) is slightly higher than the control geopolymer (0.1%). Similar to the density properties, the underwater geopolymer is also observed to provide relatively lower value (2082.92 kg/m<sup>3</sup>) compared to the control geopolymer (2168.08 kg/m<sup>3</sup>). Based on the result obtained, it is safe to say that the underwater geopolymer comprises of less compact with structure that is more porous thus lower strength when compared to the control geopolymer.

### 3.2. Microstructure (SEM/EDX)

The microstructure of the kaolin/fly ash based for underwater geopolymer and control geopolymer samples is presented in Figure 1. The higher strength geopolymer is shown in Figure 1(a) and lower strength in Figure 1(b). It is found that the underwater geopolymer have more unreacted fly ash and porosity as marked visibly in the figure. While the control geopolymer reveal to have denser matrix when compared to underwater geopolymer.

**Figure 1.** Morphology of a) control geopolymer and b) underwater geopolymer

The average content of main elements (atomic %) and the ratios in the matrix of the underwater geopolymer (UWG) and control geopolymer (CG) are given in the Table 4. The result of EDX analysis showed that the reaction of geopolymerization products consist of Si, Al, Na and Ca, which is correlated to sodium aluminosilicate hydrate (N-A-S-H) and calcium silicate hydrate (C-A-S-H) [25]. An additional of small amount element, Cl in underwater geopolymer proves the presence of chloride penetration caused by curing underwater.

**Table 4.** The average content of element (atomic %) and their ratio in the matrix of geopolymer samples.

Sample	Si	Al	Na	Ca	Fe	Cl	Mg	Al/Si	Na/Si	Na/Al	Ca/Si
UWG	12.27	6.75	4.14	4.45	4.43	0.26	3.11	0.55	0.34	0.61	0.36
CG	10.58	5.96	6.17	7.48	3.81		2.22	0.56	0.58	1.04	0.71

Typically, higher Al/Si ratio indicates higher proportion of incorporated Al in the N-A-S-H gel [26]. Thus will contribute to the formation of more homogeneous and cross-linked N-A-S-H gel resulting to

a more compacted structure and better strength development [27]. Another ratio that worth the attention are Ca/Si. The presence of Ca element produces C-A-S-H gel during the geopolymerization. Thus, both sample most probably contain of coexisting N-A-S-H and C-A-S-H gel that leads to a better compactness due the cross-linked structure. Since the Ca/Si ratio of control geopolymer is higher, it is likely expected to present higher strength compared to underwater geopolymer.

### 3.3. Elemental Distribution ( $\mu$ -XRF)

The figure 2 illustrate the imaging of Si, Al and Ca distribution confirmed by  $\mu$ -XRF analysis. Relevant to the EDX result, it is proved that the content of Ca in control geopolymer presents the highest concentration. Although the control geopolymer presents lower value of Si and Al, both amount of element is equivalent to each other thus can still produce higher ratio of Al/Si compared to the underwater geopolymer such shown in the previous table 4.

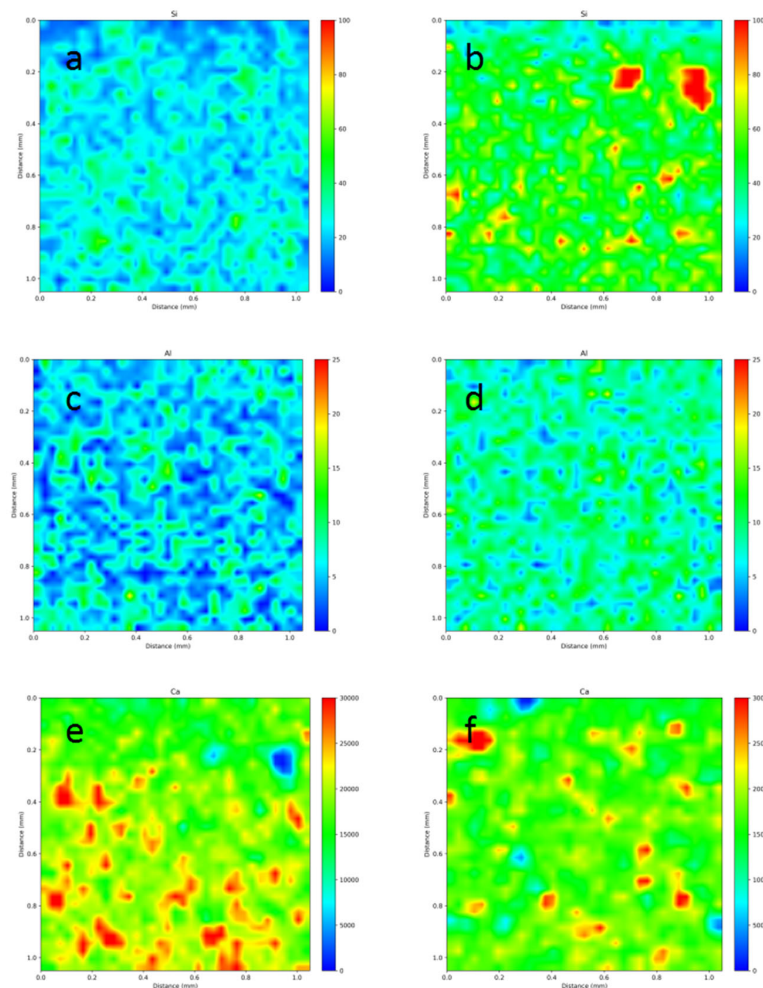


**Figure 2.** Imaging of elemental distribution of element Si for a) control geopolymer and b) underwater geopolymer, Al for c) control geopolymer and d) underwater geopolymer, and Ca for e) control geopolymer and f) underwater geopolymer.

#### 4. Conclusions

In this study, the effect of using geopolymer as underwater material is investigated. The result obtained from water absorption test, density test, microstructure analysis and elemental distribution are relevant to the strength of each sample. Although there is a reduction in the strength of underwater geopolymer compared to the control geopolymer, it can still be considered as a suitable material for underwater concreting since it is able to retain 92.02% of the control sample.

#### References

- [1] Fediuk R 2018 *Key Eng. Mater.* **769**, pp. 3–8, Apr.
- [2] Mehta J, Pitroda J and Bhavsar J J 2015 Open Caisson: Underwater Construction Technique and Placement p 1
- [3] Mikhasek A A and Rodionov M V 2015 *Procedia Eng* **111** p 516
- [4] Han B, Zhang L, and Ou J 2017 *Non-Dispersible Underwater Concrete in Smart and Multifunctional Concrete Toward Sustainable Infrastructures* (Singapore: Springer Singapore) p 369
- [5] Izzat A M, Al Bakri A M M, Kamarudin H, Sandu A V, Ruzaidi G C M, Faheem M T M, Moga L M 2013 *Revista de Chimie* **64** (9) p 1011
- [6] Albitar M, Mohamed Ali M S, Visintin P, and Drechsler M 2017 *Constr. Build. Mater* **136** p 374
- [7] Faheem M T M, Al Bakri A M M, Kamarudin H, Binhussain M, Ruzaidi C M, Izzat A M 2013 *Adv. Mater Res* **627** p 878
- [8] Liyana J, Mustafa Al Bakri A M, Kamarudin H and Aeslina A K 2018 *IOP Conf. Series: Mater. Sci. and Eng.* **374** 012046
- [9] Mustafa Al Bakri A M, Izzat A M, Faheem M T M, Kamarudin H, Khairul Nizar I, Binhussain M, Rafiza A R, Zarina Y and Liyana J 2013 *Adv. Mater. Res.* **626** 918
- [10] Ahmad R, Al Bakri A M M and Nur Ain J 2014 *Mater. Sci. Forum* **803** p 37
- [11] Fifinatasha S N, Mustafa Al Bakri A M, Kamarudin H, Zarina Y, Rafiza A R and Liyana J 2013 *Adv. in Environ. Bio.* **7** 3835
- [12] Liyana J, Mustafa Al Bakri A M, Kamarudin H, Ruzaidi C M and Azura A R 2014 *Key Eng. Mater.* **594** 146
- [13] Supriadi W, Subaer, Bayuaji R, Burhan R Y P, and Fansuri H 2016 *Mater. Sci. Forum* **841** p 178
- [14] Bayuaji R. 2014 *Mater. Sci. Forum* **803** p 49
- [15] Ruzaidi C M, Kamarudin H, Shamsul J B, Mustafa Al Bakri A M and Liyana J 2013 *Appl. Mech and Mater.* **313** 174
- [16] P Y Fauziah, M Fathullah, M M A Abdullah, Meor Ahmad Faris, Faheem Tahir, Z Shayfull, S M Nasir, M Shazzuan and A Z W Wazien 2018 *AIP Conference Proceedings.* **2030** 020067
- [17] Abdullah M M A B, Nordin N, Tahir M F M, Kadir, A A, Sandu A V 2016 *Int J Conservation Sci* **7** (3) p 753
- [18] Mustafa Al Bakri A M, Norazian M N, Mohamed M, Ruzaidi C M and Liyana J 2013 *Appl. Mech. Mater.* **421** 390
- [19] Aziz I H, M Abdullah, H Yong, L Ming, D Panias and K Sakkas 2017 *IOP Conference Series: Materials Science and Engineering* IOP Publishing p 012040
- [20] Chindaprasirt P, Phoo-ngernkham T, Hanjitsuwan S, Horpibulsuk S, Poowancum A and Injorhor B 2018 *Case Stud. Constr. Mater* **9** p 198
- [21] Aziz I H, M M A B Abdullah, H C Yong, L Y Ming, K Hussin, A A Kadir and E A Azimi 2016 *MATEC Web of Conf.* EDP Sciences p 01023
- [22] Huseien G F, Mirza J, Ismail M, Ghoshal S K, and Ariffin M A M 2018 *Ain Shams Eng. J.* **9** (4) p 1557
- [23] Muhammad Faheem M T, Mustafa Al Bakri A M, Kamarudin H, Ruzaidi C M, Binhussain M and Izzat A M 2013 *International Review of Mechanical Engineering* **7** (1) p 161
- [24] Luhar S and Khandelwal U 2015 *SSRG Int. J. Civ. Eng.* **2** **8** p 10
- [25] Azimi E, Abdullah M, Ming L, Yong H, Hussin K and I H Aziz 2016 *MATEC Web of Conf.* EDP

Sciences p 01090

- [26] Marjanović N., Komljenović M, Bašćarević Z, and Nikolić V 2015 *Procedia Eng* **108** p 231
- [27] Tamizi S M, Mustafa Al Bakri A M, Kamarudin H, Ruzaidi C M, Liyana J and Aeslina A K 2014 *Key Eng. Mater.* **594** 401